

A Log-Polar Mapping Approach to Copyright Protection of Video Data

David S. Ongoma,
Jomo Kenyatta University of Agriculture and
Technology,
Nairobi, Kenya.

Muliaro Wafula,
Jomo Kenyatta University of Agriculture and
Technology,
Nairobi, Kenya.

Tobius Mwalili,
Jomo Kenyatta University of Agriculture and Technology,
Nairobi, Kenya

Abstract:- Multimedia content is largely visual and has been prone to copyright infringement. While advocating for visualization of data and information, there is a need to ensure that such products are protected. Numerous watermarking techniques, for the protection of digital content, exist but still are not able to adequately prevent compromization of security. To achieve the desired level of security, an improved watermarking has been developed that can withstand a spectrum of possible attacks such as file compression, aspect ratio changes, filtering, cryptographic and statistical attacks. Many existing watermarking methods do not perform well against affine transformation attacks that render the watermark, to a greater extent irretrievable or undetectable.

This paper presents the Log-polar mapping approach that has demonstrated the capacity of building a domain that is invariant to affine transformation attacks. Validation of this new approach to watermarking that uses a new filtering method to find the rotation and translation parameters is shown and explained. The validation was performed by simulation using MATLAB software. Comparison of performance of the Log-polar mapping approach algorithm with other existing algorithms was done using PSNR (Peak Signal to Noise Ratio) values and results presented that were in favour of the newly developed Log-polar mapping Algorithm.

Keywords:- Multimedia, Log-polar Mapping Algorithm, MATLAB, Watermarking, Security.

I. INTRODUCTION

Progress in digital data processing has resulted in numerous merits into the data transmission, copying, storage etc. However, some advantages can be disadvantages in other ways. The easy processing of digital multimedia has caused that the illegal digital copy can be made in exactly the same quality as the original, may be created at low cost and can be transmitted very easily through the internet [3]. These reasons have established the question of ownership rights protection of

multimedia content. Two approaches are used to protect multimedia data, as stated by Arnold *et al* [4]. They include multimedia protection during transmission and multimedia protection after transmission. Multimedia protection during transmission employs the use of cryptographic schemes. They only protect the multimedia only during transmission [1]. After decryption in the receiver, they are not protected any longer and data may be copied easily without quality degradation.

Protection after transmission and decryption is achieved by adding some information into the multimedia content in which the information about multimedia such as author, source etc. can be included [5], [6]. The art of hiding information into multimedia data in a robust and invisible way is called digital watermarking. Embedded information should not be detectable to the human visual system but should be detectable by a detector which is normally used during the process of watermark extraction [11].

Cryptographic and digital watermarking methods are basic methods in the field of Digital Rights Management [8]. This is a collection of techniques and technologies which enable technically enforced licensing of digital information, secure transmission, authors and ownership rights for all types of multimedia.

In digital watermarking as a tool to protect ownership rights and copy prevention, there are lots of processes carried out by unauthorized persons that aim to corrupt the embedded information. These processes are referred to as attacks. Kim *et al.* [12] categorize attacks into four groups namely:

- Removal attacks
- Affine transformation attacks
- Cryptographic attacks
- Protocol attacks

Removal attacks

They completely remove watermark information from the watermarked data without cracking the security of the watermarking algorithm. Examples include lossy compression,

quantization, re-modulation, collusion, de-noising and averaging attacks [15].

Affine transformation attacks

They do not remove the embedded watermark itself but intent to distort the watermark detector synchronization with the embedded information [19]. Examples include scaling, rotation, translation, and cropping.

Cryptographic attacks

They aim at cracking the security methods in watermarking schemes thereby finding a way to remove the embedded watermark information. They are brute force attacks which aim at finding secret information via exhaustive search [16].

Protocol attacks

They aim at attacking the whole concept of the watermarking application. They include copy attack and attacks made by invertible watermarks [12].

Affine transformation attacks in digital watermarking are still an open problem for many watermark algorithms used currently [30]. Most affine transformational attacks can be uniquely described using the paradigm of affine transforms that can be represented by four coefficients $t_{11}, t_{12}, t_{21}, t_{22}$ forming a matrix T for the linear component, plus the two coefficients t_h, t_v , for the translation part of the transform. The affine transform maps each point of Cartesian coordinates from (x,y) to (x',y') [30]. This transform can be depicted in the following form as illustrated by Ahuja & Bedi [2]:

$$\begin{aligned} \begin{Bmatrix} x' \\ y' \end{Bmatrix} &= T_x \begin{Bmatrix} x \\ y \end{Bmatrix} + t \\ &= \begin{Bmatrix} t_{11} & t_{12} \\ t_{21} & t_{22} \end{Bmatrix} * \begin{Bmatrix} x \\ y \end{Bmatrix} + \begin{Bmatrix} t_x \\ t_y \end{Bmatrix} \end{aligned} \tag{1}$$

where “ \times ” represents the matrix product. The t component corresponds to the cropping and the translation. The different values of the t_{ij} components in the matrix T represent the different types of the affine transforms. According to Ahuja & Bedi [2], the parameters of the transformation for a rotation $R(\theta)$ of a certain angle θ are:

$$T(\theta) = \begin{Bmatrix} \cos(\theta) & -\sin(\theta) \\ \sin(\theta) & \cos(\theta) \end{Bmatrix} ; \begin{Bmatrix} t_x \\ t_y \end{Bmatrix} = \begin{Bmatrix} h \\ v \end{Bmatrix} \tag{3}$$

For *scaling* $S(\rho)$ factors ρ_x and ρ_y applied, respectively, to the horizontal and vertical axes, the transformation parameters are:

$$T(\rho_x, \rho_y) = \begin{Bmatrix} \rho_x & 0 \\ 0 & \rho_y \end{Bmatrix} ; \begin{Bmatrix} t_x \\ t_y \end{Bmatrix} = \begin{Bmatrix} 0 \\ 0 \end{Bmatrix} \tag{4}$$

The parameters for *translation* $T(h,v)$ in x and y directs off a hand v pixels are:

$$T(h, v) = \begin{Bmatrix} 1 & 0 \\ 0 & 1 \end{Bmatrix} ; \begin{Bmatrix} t_h \\ t_v \end{Bmatrix} = \begin{Bmatrix} h \\ v \end{Bmatrix} \tag{5}$$

Fundamental Terminologies

In this section, important terminologies which are required to understand the thesis are introduced.

• *Translation*

A translation is applied to the frame of an image or video by repositioning it along a straight-line path from one coordinate location to another. We translate a 2-D point by adding translation distances, x_0 and y_0 to the original coordinate position (x, y) to move the point to a new position

$$\begin{aligned} (x', y') & [27]. \\ x' &= x+x_0, y' = y+y_0 \end{aligned} \tag{6}$$

The translation distance pair (x_0, y_0) is known as a translation vector.

• *Scaling*

A scaling transformation changes the size of an image. Transformation equations are obtained by multiplying the coordinate values (x, y) by scaling factors σ_x and σ_y to produce the transformed coordinates (x', y') as shown below:

$$\begin{aligned} x' &= x.\sigma_x \\ y' &= y.\sigma_y \end{aligned} \tag{7}$$

Scaling factor σ_x scales images in the x direction, while σ_y scales in the y direction. When σ_x and σ_y are assigned the equal value, a uniform scaling maintains the relative image proportions [27].

• *Rotation*

A 2-D rotation is applied to an image frame or video frame by repositioning it along a circular path in the xy plane. The transformation equations for rotating a point at (x, y) are obtained through an angle α about the origin counter clockwise as shown below:

$$x' = x \cos \alpha + y \sin \alpha, y' = -x \sin \alpha + y \cos \alpha \tag{8}$$

II. THE PROPOSED SCHEME

An efficient video watermarking scheme is presented based on Log Polar Mapping and a new filtering method. The raw videos are divided into groups of pictures with a fixed length. Fourier transform is applied to the frame of each group of pictures. Then, the log-polar mapping is applied to the magnitude of the Fourier spectrum. The proposed filter is used to find the parameters of rotation and scaling for a frame that has undergone an affine transform attack. This is illustrated in figure 1.

Image registration method suggested by Wu and Liu [39] is used with a small template cut from the original frame to find the watermark locations. The new filtering method is applied for template matching. Then, the distorted frame is resynchronized during the watermark detection process. The method is very robust to MPEG-2 compression and affine transform attacks.

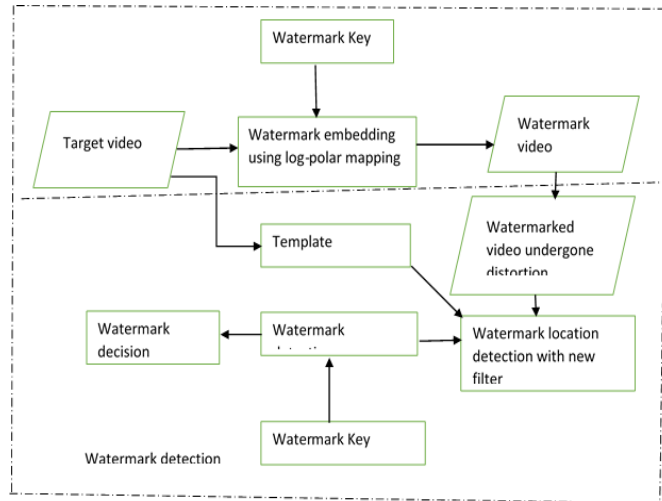


Fig 1:-Proposed scheme

III. FILTERS

Phase-only filter offers a better performance compared to classical matched filter. It has high correlation peaks and provides a higher discrimination capability. However, this filter has a low SNR and is more sensitive to distortions [24].

• Filters evaluation

Filters are evaluated based on the following measures:

Assume $f(x)$ is a signal in the object plane and $F(u)$ is its complex Fourier transform. Also, let $n(x)$ be a sample that has been realized from a zero-mean stationary random process with a power spectral density $P_n(u)$. $n(x)$ and $f(x)$ can be used as inputs to a linear space-invariant system with an impulse response $h(x)$ and its corresponding transfer function $H(u)$. $g(x)$ will be the output of the signal while $G(u)$ will be its complex Fourier representation.

Three measures are used to evaluate the performance of filters/correlators. They include signal-to-noise ratio (SNR), correlation peak intensity (CPI) and light efficiency (LE).

A. Signal-to-noise Ratio (SNR)

SNR is the ratio of the strength of an electrical or other signal carrying information to that of unwanted interference. It is defined as:

$$SNR = |g(0)|^2 / \sigma^2 \tag{9}$$

Where $g(0)$ is the output sampled at $x=0$ and σ^2 is the variance of noise.

SNR in the frequency domain is given by:

$$SNR = \frac{|\int F(u)H(u)du|^2}{\int P_n(u)|H(u)|^2 du} \tag{10}$$

The integration limits are from $-\infty$ to $+\infty$. Filters that yield a higher SNR have a better detection performance.

Filters that yield higher SNR values have a better detection performance.

B. Correlation Peak Intensity (CPI)

It is the light intensity at the origin ($x=0$) in the output plane and is given by:

$$CPI = |g(0)|^2 \tag{11}$$

CPI in the frequency domain is given by:

$$CPI = |\int F(u)H(u)du|^2 \tag{12}$$

The integration limits are from $-\infty$ to $+\infty$.

The higher the CPI the better the ability to detect light at the output plane.

C. Light Efficiency (LE)

It is the amount of visible light emitted for a given amount of power used.

It is defined as:

$$LE = n_m \left[\frac{\int |G(u)|^2 dx}{\int |f(x)|^2 dx} \right] \tag{13}$$

Where n is the light efficiency and n_m the medium or diffraction efficiency. The limits of integration are from $-\infty$ to $+\infty$, hence an n_m .

In frequency domain, the equation can be written as:

$$LE = n_m \frac{\int |G(u)|^2 du}{\int |F(u)|^2 du} = n_m \frac{\int |F(u)H(u)|^2 du}{\int |F(u)|^2 du} \tag{14}$$

• The Proposed Filter

The proposed filter improves the SNR of the phase-only filter by limiting its bandwidth. Assume that the reference signal $f(x)$ is such that the signal Fourier transform's magnitude $|F(u)|$ is zero for all $|u|$, this filter is defined using the equation below:

$$H(u) = \begin{cases} \exp(-j\varphi F(u)) & \text{if } |u| \leq u_h; \\ 0 & \text{otherwise} \end{cases} \tag{15}$$

Where the filter bandwidth u_h is less or equal to the signal bandwidth u_f .

Performance measures

SNR

Replacing the expression for $H(u)$ given by equation (15) in equation (10), SNR for this proposed filter is calculated as shown below:

$$SNR = \frac{|\int_{-u_h}^{u_h} F(u)du|^2}{\int_{-u_h}^{u_h} P_n(u)du} = 2 \frac{|\int_0^{u_h} F(u)du|^2}{\int_0^{u_h} P_n(u)du} \tag{16}$$

The even symmetry of $|F(u)|$ and $P_n(u)$ is used.

Correlation peak Intensity

The CPI is obtained by substituting equation (15) in equation (12) as shown below:

$$CPI = 4 \left| \int_0^{u_h} |F(u)|^2 du \right|^2 \tag{17}$$

Light Efficiency

Substituting equation (14) in equation (15), the light efficiency of the filter is obtained as follows:

$$LE = \frac{\int_0^{u_h} |F(u)|^2 du}{\int_0^{u_h} |F(u)|^2 du} \tag{18}$$

IV. WATERMARK INSERTION

- Insert a watermark sequence into the log-polar mapping domain of each video frame.
- Divide the target video clips in into groups of 16 frames each.
- Truncate the frames into smaller squares of size 480 by 480 pixels, to make them more tolerant to rotation and cropping attacks in log-polar mapping domain, as compared to rectangular ones [35].
- Calculate the discrete Fourier transform of the truncated frames.
- Save a block portion of the log-polar mapping spectrum as the matching template, to be used during extraction of the watermark and detection of the transformations undergone by the frame.
- Select the desirable positions in the log-polar magnitude spectrum to embed the watermark.
- Embed the watermark in the inverse log-polar map spectrum. If the watermark was to be embedded in the log-polar mapping domain, inverse log-polar mapping will be required to transform back the log-polar mapping domain to the discrete Fourier transform domain [32].

Use the below formula to insert the watermark:

$$A = A' + B * C \tag{19}$$

where A is the original image's DFT amplitude spectrum, A' is the modified DFT amplitude spectrum of the original image, B is the watermarking strength that is used to achieve the tradeoff between the visibility of the watermark and its robustness, and C is the watermark data.

- Apply inverse DFT to the watermarked frame.
- Select the middle-frequency components as the positions to insert the watermark data, since the closer the center the higher the sampling rate [38].

The steps for embedding the watermark are shown in the figure below:

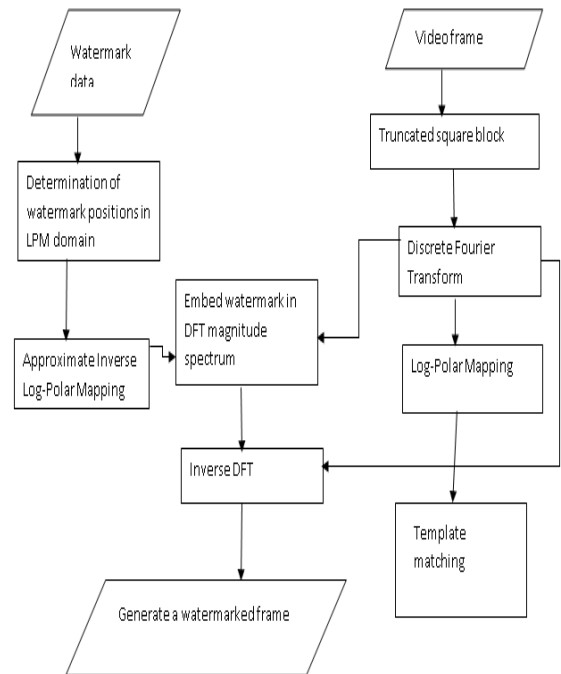


Fig 2:-Watermark insertion

V. WATERMARK EXTRACTION

- Apply DFT and log-polar mapping to each truncated watermarked frame and transform it to the log-polar domain.
- Calculate the correlation between the matching template and the watermarked frame using the new proposed filter.
- Find the peak of the calculated correlations together with the translations.
- Calculate the coordinates of the new watermark position in the watermarked image that have undergone attacks using the equations below:

$$\begin{aligned} \rho w_i' &= \rho w_i + \Delta \rho \\ \theta w_i' &= \theta w_i + \Delta \theta \end{aligned} \tag{20}$$

where the coordinates of the original watermark w_i are $(\rho w_i, \theta w_i)$.

- Retrieve the watermarked data W' at the corrected position using the formula below:

$$W' = \frac{E'}{B} \tag{21}$$

Where E' is the DFT magnitude spectrum of the watermarked frame that has undergone attacks and B is the watermarking strength that is used to achieve the tradeoff between the visibility of the watermark and its robustness.

- Calculate the normalized correlation coefficient between the original watermarked data and the extracted watermarked data using the equation below:

$$NC = \frac{W * Vt}{\sqrt{(W * Wt)(V * Vt)}} \tag{22}$$

Where W is the vector of the original watermark, V is the vector of the retrieved watermark, and $(.)^T$ is the transpose operation of a matrix. The watermark extraction procedure is shown in the figure below:

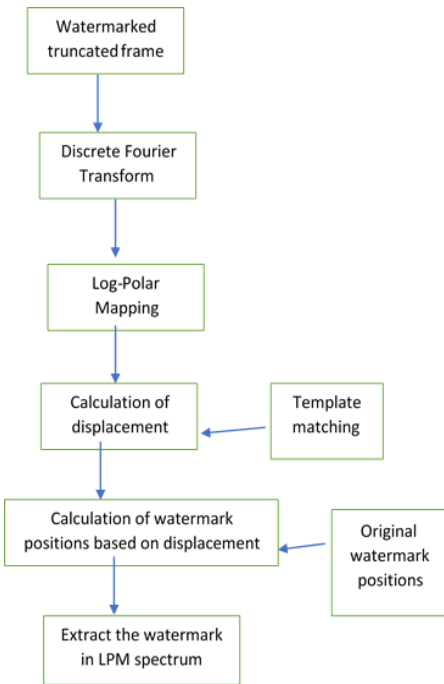


Fig 3:-Watermark extraction

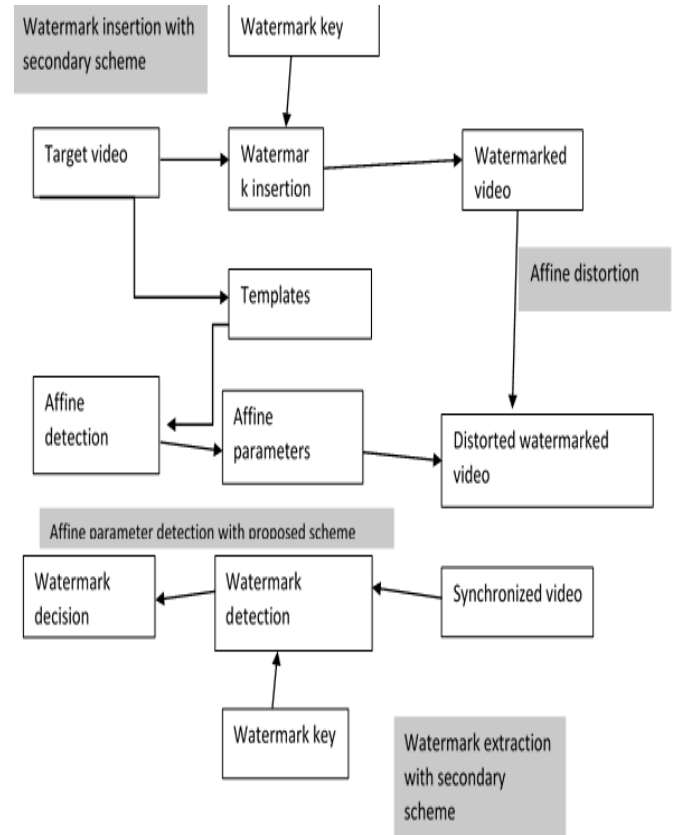


Fig 4:-Integration of the proposed scheme with other algorithms

VI. INTEGRATION OF THE PROPOSED SCHEME WITH OTHER ALGORITHMS

The proposed scheme based on log-polar mapping and the new filter is capable of withstanding affine transform attacks. Embedding and extraction of the watermark were performed in the log-polar mapping domain. The normalized cross-correlation was used to detect the existence of a watermark in the target videos [36]. The scheme can also detect rotation, translation and scale parameters that the video has undergone, hence it can work alongside other algorithms as a parameter detector for rotation, scaling, and translation. The figure 4 below portrays how the scheme can be integrated with other algorithms as a parameter detector. The scheme will work independently from the watermark embedding and detection of the other watermarking scheme. The proposed scheme will be integrated into a fragile scheme to enhance its robustness to affine attacks/distortions.

VII. DETECTION OF AFFINE PARAMETERS

The proposed scheme can withstand affine transformation attacks due to its capability to detect and calculate the exact rotation angle, translation parameters and the scaling ratio of the target videos. The scheme uses the new proposed filter that gives the best discrimination for the cross-correlation between the template and the target video frame. This feature makes it possible to use this scheme with other watermarking schemes to detect affine parameters, as portrayed in the figure 5 below.

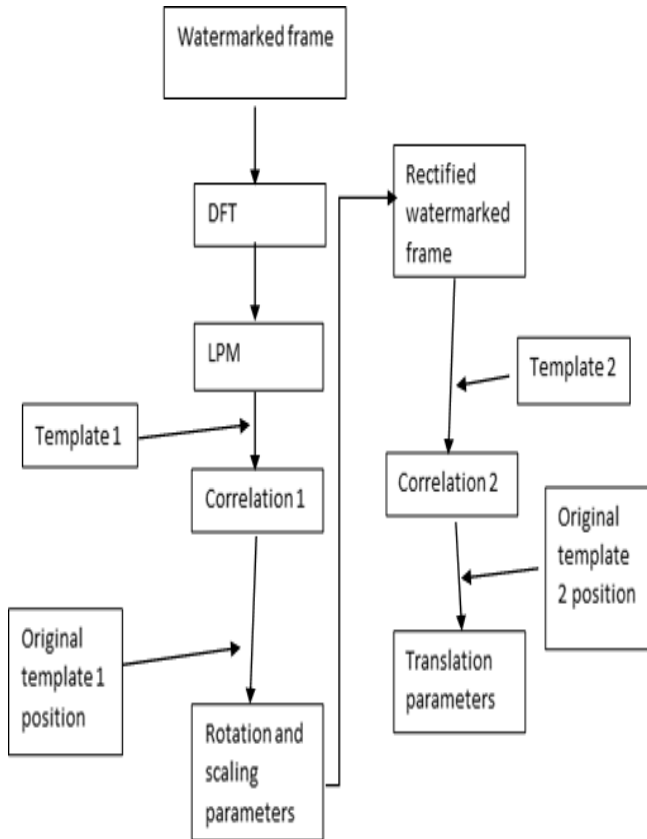


Fig 5:-Detection of affine parameters

VIII. COMPUTING SCALING AND ROTATION PARAMETERS

From the diagram above in figure 5, the initial template is used in the log-polar mapping domain to detect the position of the current watermark and also to get the parameters for scaling and rotation. The location of the matching template in the log-polar domain that has undergone affine transform attacks is the peak in the correlation spectrum.

Assuming that the peak coordinate is (ρ_1, θ_1) and the original position of the first template is (ρ_0, θ_0) , then the translations in the log-polar domain will be as shown in equation (23) below:

$$\begin{aligned} \Delta_\rho &= \rho_1 - \rho_0 \\ \Delta_\theta &= \theta_1 - \theta_0 \end{aligned} \tag{23}$$

Δ_ρ and Δ_θ represent the number of pixels that are shifted respectively along the ρ and θ axis. These pixels correspond respectively to the parameters of rotation and scaling in the spatial domain. These parameters can be calculated according to the equation (24) below:

$$\begin{cases} \alpha' = \frac{360^\circ \cdot \Delta\theta}{N'} \\ \sigma' = e^{\frac{\ln(rmax) \cdot \Delta\rho}{M'}} \end{cases} \tag{24}$$

Where $rmax = \sqrt{(\frac{M'}{2})^2 + (\frac{N'}{2})^2}$

α' and σ' are the rotation and scaling ratio respectively in the spatial domain computed from Δ_ρ and Δ_θ in the log-polar mapping domain. M' and N' are the number of pixels along the ρ and θ axis in log-polar domain respectively, and the size of the log-polar mapping domain is $M' \times N'$ while $M \times N$ is the size of the magnitude spectrum of the Fourier transform.

IX. COMPUTING TRANSLATION PARAMETERS

Since the magnitude of a video frame's Fourier transform is independent of the translation parameters, the translational parameters in the spatial domain are the ones to be calculated, not of the Fourier transform domain. Another block is cut in the spatial domain as the second template and the cross-correlation between this second template and the watermarked frame that has undergone affine transform attacks is calculated using the proposed new filtering method. Assuming that the peak coordinate is (x_1, y_1) and the template's original position is (x_0, y_0) , the translation parameters are computed as follows:

$$\begin{cases} \Delta x = x_1 - x_0 \\ \Delta y = y_1 - y_0 \end{cases} \tag{25}$$

It's so simple to invert the translation transform that has been applied to the watermarked frame. The detected translation parameter is precise since the values that have been detected are to the real parameters of translation.

X. RESULTS AND DISCUSSION

- *Performance Evaluation of the proposed filter using 2D Signals*

The proposed filter is synthesized to detect a specific pattern in the input plane. A rectangular block padded with zeros to form an image of size 128 by 128 pixels is used as a reference pattern in the simulations. The pixel values for the image are coded in binary using two levels. The images that are input are subjected to several noise levels.

	Classical Matched Filter	Phase-Only Filter	Proposed Filter
N(0, 0) No noise	0.061	1.000	0.077
N(0, 1)	0.050	1.000	0.063
N(0, 2.25)	0.041	1.000	0.053
N(0, 4)	0.031	1.000	0.043

Table 1. Correlation Peak Intensities. All the values have been normalized to those of the Phase-Only Filter

The noise applied is zero-mean and Gaussian white noise of 1, 1,2.25 and 4 variances. Correlations were performed 2-D Fast-Fourier Transforms of 128 by 128 in size. Simulations were also carried on the classical matched filter and phase-only filter for comparison. Computation for the correlation plane was performed and CPIs for the filters at several noise cases recorded as shown in table 1.

The phase only filter offers the best correlation peak intensities as shown in table 1. CPI is important in some space type of applications where the light power is limited.

The signal to noise ratios, SNR was also computed using the equation below:

$$SNR = \frac{[\sum_{k=1}^d |F(k)||H(k)|]^2}{No[\sum_{k=1}^d |H(k)|^2]} \quad (26)$$

	Input Signal to noise ratio	Classical Matched Filter	Phase-Only Filter	Proposed Filter
N(0, 0) No noise	-	-	-	-
N(0, 1)	44.09	64.20	54.27	62.63
N(0, 2.25)	37.05	60.67	50.75	59.11
N(0, 4)	32.05	58.18	48.25	56.61

Table 2. SNR in decibels

From the above results, it's clear that the classical matched filter provides the best SNR compared to the other filters under various noise cases. SNR gain is important in cases where the likelihood of erroneous detection is probably in the presence of noise.

• *Simulation results for the proposed scheme*

The performance of the proposed method is illustrated in this section. 5 test videos are used.

Rotation

The table 3 below shows results watermarked and unwatermarked videos that have been rotated up to 45°. From the table, similarity values for watermarked videos are much higher than that for unwatermarked videos, suggesting that this method is robust to the rotation. W stands for watermarked video while U stands for unwatermarked video.

Rotation angle in degrees	Video 1 704 by 576		Video 2 704 by 480		Video 3 704 by 480		Video 4 704 by 576		Video 5 704 by 480	
	W	U	W	U	W	U	W	U	W	U
PSNR	39.8486	-	39.4480	-	39.1571	-	39.8101	-	40.3352	-
0	0.9547	0.0935	0.9976	0.2455	0.9706	0.2069	0.9957	0.0235	0.9806	0.3119
5	0.8801	0.1238	0.8752	0.2288	0.8490	0.1639	0.8940	0.1149	0.8059	0.3087
10	0.7995	0.2675	0.90470	0.2987	0.8643	0.1464	0.8659	0.0375	0.8227	0.4211
15	0.8668	0.2391	0.8636	0.2618	0.8126	0.1899	0.8626	0.0919	0.8621	0.2584
20	0.7886	0.2048	0.9207	0.3664	0.8178	0.1508	0.8461	0.2497	0.8072	0.1838
25	0.8346	0.2614	0.9246	0.3020	0.8430	0.1110	0.7874	0.2658	0.8522	0.2763
30	0.8125	0.2764	0.4543	0.4347	0.7300	0.4203	0.8649	0.2944	0.7607	0.3414
35	0.7804	0.2258	0.9174	0.1106	0.8727	0.2018	0.8469	0.2836	0.7235	0.3069
40	0.6880	0.2772	0.9022	0.1695	0.8080	0.3389	0.7977	0.3089	0.7038	0.3236
45	0.5452	0.0976	0.8994	0.2336	0.6722	0.1684	0.8159	0.2152	0.6054	0.2589

Table 3. Similarity results for rotated videos

The results were plotted on the graph in figure 3 above.

Scaling

Scaling ratios from 80% to 130% are considered. The bilinear interpolation method is used to resize each frame of the target video into a scale size. The results were tabulated in Table 4.7.2 below. From the table, the similarity values for

watermarked videos. was much higher than for the unwatermarked videos, hence, it was easier to tell if the video was watermarked or not.

This shows that the proposed method can withstand scaling attacks.

Scaling in percentage	Video 1 704 by 576		Video 2 704 by 480		Video 3 704 by 480		Video 4 704 by 576		Video 5 704 by 480	
	W	U	W	U	W	U	W	U	W	U
PSNR	39.8486	-	39.4480	-	39.1571	-	39.8101	-	40.3352	-
80	0.8894	0.2352	0.8603	0.2619	0.8976	0.0538	0.8528	0.1566	0.7510	0.2506
90	0.8694	0.0548	0.9694	0.1891	0.9140	0.0566	0.8677	0.1213	0.8554	0.2014
110	0.8534	0.1354	0.9746	0.2781	0.9034	0.0458	0.9401	0.1999	0.9313	0.1603
120	0.7959	0.1247	0.9622	0.1936	0.9515	0.1473	0.9322	0.1834	0.9166	0.1819
130	0.7434	0.1494	0.9655	0.3152	0.8921	0.1460	0.7989	0.1756	0.7286	0.3522

Table 4. Similarity results for scaled videos

Translation

Translation results were tabulated in Table 4.7.3 below. The table shows that the similarity results are almost the same

regardless of how many pixels the translations occurred to the watermarked video.

	Video 1 704 by 576		Video 2 704 by 480		Video 3 704 by 480		Video 4 704 by 576		Video 5 704 by 480	
	W	U	W	U	W	U	W	U	W	U
PSNR	39.8486	-	39.4480	-	39.1571	-	39.8101	-	40.3352	-
Translation	0.9470	0.1270	0.9944	0.1232	0.9440	0.2122	0.9834	0.1258	0.9496	0.1524

Table 5. Similarity results for translated videos

Combined affine transform attacks

The Table 4.7.4 below shows the combined affine attacks where rotation is by 150, translation by 50 pixels and

scaling by 110%. The results show that the proposed scheme is robust to affine transform attacks.

	Video 1 704 by 576		Video 2 704 by 480		Video 3 704 by 480		Video 4 704 by 576		Video 5 704 by 480	
	W	U	W	U	W	U	W	U	W	U
PSNR	39.8486	-	39.4480	-	39.1571	-	39.8101	-	40.3352	-
Combined affine transform	0.7568	0.2856	0.8886	0.3181	0.7362	0.2781	0.7610	0.2322	0.7211	0.2397

Table 6. Similarity results for translated, scaled and rotated videos

XI. CONCLUSION AND FUTURE WORK

In this paper, we propose a video watermarking scheme based on log-polar mapping and a new filtering technique. The paper applies the idea that log polar domain is invariant to rotation, cropping, shearing, translation and scaling transformations. The template is used to find the location of the watermark. The new filter proposed is used for template matching and detecting the parameters of translation, rotation and scaling which are used by the scheme to be integrated with other schemes to make them more resistant to attacks. Test results have clearly shown that the algorithm is very invariant to affine transformation attacks. The scheme is also capable of being integrated into other weak schemes to strengthen their resistance to rotation, translation and scaling attacks.

In future, we intend to refine the scheme to make it more resistance to H.264 which is the most advanced video compression standard.

REFERENCES

- [1] Abdullah, M., Elrowayati, A., & Manaf, A. "Recent Methods And Techniques In Video Watermarking And Their Applicability To The Next Generation Video Codec" Journal Of Theoretical And Applied Information. Technology, 2015.
- [2] Ahuja, R., & Bedi, S. "All Aspects of Digital Video Watermarking Under an Umbrella" Online, 2015.
- [3] Al-Haj, A. "Advanced techniques in multimedia watermarking: Image, video, and audio applications" Hershey, PA: Information Science Reference, 2010.
- [4] Arnold, M., Schmucker, M., & Wolthusen, S. "Techniques and Applications of Digital Watermarking and Content Protection" Techniques and Applications. Norwood: Artech House, 2013.

- [5] Bhattacharyya, S., Bhaumik, H., De, S., & Klepac, G. Analysis of Multimedia Information. Hershey: IGI Global, 2016.
- [6] Cox, I., Miller, M., & Bloom, J. Digital Watermarking. Burlington: Elsevier, 2001.
- [7] Cvejic, N., & Seppanen, T. Digital audio watermarking techniques and technologies: Applications and benchmarks. Hershey: Information Science Reference, 2008.
- [8] Dhar, P., & Shimamura, T. Advances in audio watermarking based on singular value decomposition, 2015.
- [9] Furht, B., Muharemagic, E., & Socek, D. Multimedia Encryption and Watermarking. Boston, MA: Springer Science+Business Media, Inc, 2013.
- [10] Hassanien, A. Multimedia forensics, and security. SI: Springer International Pu, 2016.
- [11] Ho, A. T. Digital watermarking: 8th international workshop; proceedings. (Digital Watermarking.). Berlin: Heidelberg, 2009.
- [12] IWDW (Conference), Kim, H., Katzenbeisser, S., & Ho, A. Digital watermarking: 7th international workshop, IWDW 2008, Busan, Korea, November 10-12, 2008: selected papers. Berlin: Springer, 2009.
- [13] Jackson, S. Research methods, and statistics: A critical thinking approach. Belmont, CA: Wadsworth Cengage Learning, 2012.
- [14] Kamel, M., Campilho, A., & International Conference [on] Image Analysis. analysis and recognition: Second International Conference, ICIAR 2013. Canada: Springer, 2013.
- [15] Katzenbeisser, S., & Petitcolas, F. Information hiding techniques for steganography and digital watermarking. London: Artech House, 2009.
- [16] Kumar, M., Gupta, S., & Henseman, A. Catalog of Hybrid Video Watermarking Techniques (9th ed., Vol. 143). International Journal of Computer Applications, 2016.
- [17] Lu, W., & International Conference on Information Technology. Proceedings of the 2012 international conference on information technology and software engineering: Software engineering & digital media technology. Berlin: Springer, 2013.
- [18] Mostafa, S., & Ali, A. Multiresolution Video Watermarking Algorithm Exploiting the Block-Based Motion Estimation. Journal of Information Security, 260-268, 2016.
- [19] Nagamalai, D., Renault, E., & Dhanuskodi, M. Advances in digital image processing and information technology: Proceedings. Berlin: Springer, 2011.
- [20] Naskar, R., & Chakraborty, R. Reversible digital watermarking: Theory and practices. SI: Morgan & Claypool, 2014.
- [21] Nematollahi, M. A., Vorakulpipat, C., & Rosales, H. G. Digital watermarking: Techniques and trends, 2016.
- [22] Pan, J., Huang, H., & Jain, L. Intelligent watermarking techniques. River Edge, N.J: World Scientific, 2014.
- [23] Rajab, L., Al-Khatib, T., & Al-Haj, A. A Blind DWT-SCHUR Based Digital Video Watermarking Technique. Scientific Research Publishing, 2014.
- [24] Rao, C., & Prasad, M. watermarking techniques in curvelet and ridgelet domain.
- [25] Seitz, J. (2010). Digital watermarking for digital media. Hershey, Pa: Information Science Pub, 2016.
- [26] Sengupta, S., Das, K., & Khan, G. Trends in Computing and Communication. New Delhi: Springer, 2014.
- [27] Shi, Y., Kim, H., & International Workshop on Digital Watermarking. Digital watermarking: 6th international workshop, IWDW 2007, Guangzhou, China, December 3-5, 2014: proceedings. Berlin: Springer, 2014.
- [28] Shih, F. Processing, and pattern recognition: Fundamentals and techniques. Piscataway, NJ: IEEE Press, 2010.
- [29] Tasič, J., Najim, M., & Ansoerge, M. Intelligent Integrated Media Communication Techniques. Boston: Springer Science + Business Media, Inc., 2014.
- [30] Wang, F., Pan, J., & Jain, L. in digital watermarking techniques. Berlin: Springer, 2009.
- [31] Bigun, J. Vision with direction: A systematic introduction to image processing and computer vision. Berlin: Springer, 2006.
- [32] Brunelli, R. Template matching techniques in computer vision. Chichester, U.K: Wiley, 2009.
- [33] Liu, J. Multimedia fingerprinting forensics for traitor tracing. New York, NY: Hindawi Publ. Corp, 2005.
- [34] Nakatsu, R., & Hoshino, J. Entertainment Computing: Technologies and Application. Boston, MA: Springer US, 2013.
- [35] Perales, F. Pattern recognition and image analysis. Mallorca, Spain: Springer, 2011.
- [36] Puppo, E. Image analysis, and processing. Genoa, Italy: Proceedings, 2015.
- [37] Sgallari, F., Murli, A., & Paragios, N. Scale space and variational methods in computer vision. Ischia, Italy: Springer, 2007.
- [38] Vaseghi, S. Advanced Digital Signal Processing, and Noise Reduction. Chichester: John Wiley & Sons, 2016.
- [39] Wu, M., & Liu, B. Multimedia data hiding. New York: Springer, 2013.